Hindawi
Journal of Spectroscopy
Volume 2022, Article ID 3627705, 10 pages
https://doi.org/10.1155/2022/3627705

Research Article

Investigation of Formalin-Fixed Tissue Optical Characteristics in the Range of 200–500 GHz Using Pulsed Terahertz Reflection Spectroscopy to Differentiate Oral Malignant, Benign, and Cyst

S. Stella Jenifer Isabella,[1] **K. A. Sunitha**,[1] **K. T Magesh**,[2] **Sridhar P. Arjunan**,[1] **and Bala Pesala**[3]

[1]*Department of Electronics & Instrumentation Engineering, SRM Institute of Science and Technology, Chennai, India*
[2]*Department of Oral Pathology and Microbiology, SRM Kattankulathur Dental College, SRMIST, Chennai, India*
[3]*Ayur.AI, Chennai, India*

Correspondence should be addressed to K. A. Sunitha; sunithak@srmist.edu.in

Received 24 September 2021; Accepted 20 January 2022; Published 27 February 2022

Academic Editor: Daniel Cozzolino

The application of Terahertz electromagnetic waves to diagnose oral cancer was investigated. A single case of formalin-fixed oral squamous cell carcinoma (malignant), ameloblastoma (benign), and odontogenic keratocyst was examined using terahertz pulsed spectroscopy in the frequency span of 0.1–2 THz. The measured absorption coefficient, refractive index, and the extinction coefficient were reported to be high for malignant samples than benign and cyst. The THz results are validated with hematoxylin and eosin-stained microscopic images. The results demonstrate that the THz signal was shown to be consistently higher for the malignant sample compared to benign and the cyst. These results indicate that THz signals responded to the cell density by eliminating the effect of water.

1. Introduction

Oral cancer is a term that refers to cancers of the tongue, mucosa, gingiva, salivary glands, and the floor of the mouth and palate. It is treatable with a good prognosis if detected early. However, delayed diagnosis is a major social and health care problem [1–3]. Owing to the nature of the disease and resulting morbidity, oral cancer is a major public health concern. Globally, WHO reports that 3.5 billion people are affected with oral disease [4]. India reported the highest number of oral cancer cases, with an annual diagnosis of 77000 new cases and 52000 deaths [5]. Comparatively, oral cancer is a greater issue in India than it is in the west, with 70 percent of cases being reported at an advanced stage (Stage III-IV). Only 20 percent of patients survive five years because of the late diagnosis of cancer [6].

Globally, 84–97% of oral cancer contributes to oral squamous cell carcinoma (OSCC). Oral cancer is related to tobacco use, particularly smokeless tobacco (SLT), chewing pan, poor oral hygiene, excessive alcohol use, and a nutrient-deficient diet, such as the human papillomavirus (HPV). There is significant variation in worldwide incidence owing to a variety of reasons such as a lack of knowledge, exposure to dangerous meteorological conditions, and psychological threat [7, 8].

Numerous conventional imaging modalities are used to assess, diagnose, and plan treatment for oral cancer. This includes physical and histopathological examination, staining, biopsy conventional radiography, traditional CT, magnetic resonance imaging (MRI) [9], and functional imaging using positron emission tomography (PET in combination with conventional CT [10]. Noninvasive diagnostic techniques such as visual autofluorescence play a vital role in diagnosing oral cancer. VELscope® is a non-magnifying hand-held instrument approved by the FDA in 2006 for direct visualization of oral mucosa autofluorescence

[11]. Lane et al. reported a study of 44 patients with OSCC who underwent VELscope. The results showed that the method can distinguish OSCC from normal oral mucosa with good sensitivity and specificity [12]. Future researchers intended to improve the device's specificity for wider clinical usage. Because imaging scans are difficult to interpret in diagnosing SCC, a sample of the lesion is required for histopathological testing and subtyping. Malignant tissues are often identified by biopsy, which necessitates invasive tissue sampling.

The intraoperative frozen section biopsy is commonly employed to differentiate the cancerous tissue from the normal. Manually inspecting slides stained with H&E and reviewed by pathologists for disease diagnosis are a labor-intensive and time-consuming process. But most crucially, this procedure involves subjective judgments that might be flawed and is vulnerable to huge inter- and intraobserver variations. Based on H&E-stained pictures, even highly trained pathologists have difficulty reaching a consensus on the diagnosis of cancers because of their variety and complexity. Such procedures are exact, but invasive and only performed during surgery, which results in delayed diagnosis and poor prognosis. The below Table 1 shows the various diagnosing techniques using oral tissue for the detection of oral cancer.

Table 1 summarizes the current noninvasive diagnosing techniques of the oral tissue specimen.

There is a need for a noninvasive method that can detect the presence of malignant tissues. Based on the malignant tissue property that contains more water [24], we propose the use of THz to differentiate between benign and diseased tissues. Since THz wavelengths display better penetration into fats than microwaves, they have a greater imaging resolution. Another benefit of THz imaging over other approaches is its ability to extract the spectral data from the time domain terahertz waveform through Fourier transformation. This method allows one to determine the sample's absorption coefficient and the refractive index [25, 26].

Terahertz is positioned between the microwave and infrared areas, which include frequencies span of 0.1 to 10 THz ($1\,\text{THz} = 10^{12}\,\text{Hz}$), which range from 3 mm to 30 μm analogous to wavelengths. Radiations are not ionizing, harmless for medical imagery at these frequencies [27]. However, due to the absence of effective "sources and detectors," the THz region has remained undiscovered for a long time. It was colloquially known as "THz Gap." Later, the same year, David Auston of AT & T Bell Laboratories created a photoconductive emitter gated by an optical pulse, laying the foundations for bridging the THz gap [28]. Coherent detection of THz radiation has enabled THz-TDS and its imaging techniques to explore in various fields such as pharmaceuticals, physics, astronomy, security screening, and medical imaging [29]. Indeed, biomedical research has accelerated in recent years. For instance, terahertz imaging has been used to diagnose skin cancer [30–32], breast cancer [33, 34], and colon cancer [35] as well as dental cancer [36]. Terahertz spectroscopy was also utilized for the research of protein spectroscopy [37] and the analysis of the characteristics of crystalline molecules [38], including water-protein interactions [39].

One of the fundamental works in this field has been conducted by TeraView, UK, who have reported performing long-term systemic studies on the use of THz in diagnosis of tumor. Their publications report includes THz based characterization of tissue properties, imaging of affected tissue, and the mechanism of tissue mass interaction with the THz wave.

The majority of tissues studied by THz spectroscopy are classified into three types paraffin embedded tissues [40, 41], fresh tissues [42], and frozen tissues [43, 44]. The study revealed the variations in THz frequency span of absorption coefficient and the refractive index of frozen or fresh skin, colon, and breast cancer tissues compared to normal tissue. It is mainly related with an increase in water content in a cancer tumor, which may be easily detected using THz spectroscopy [45]. However, due to the connection of numerous illnesses with excess fluid, the specificity of such criteria is not great.

To date, there have been no studies comparing absorption, refractive, and extinction coefficient of formalin-fixed oral cancer, ameloblastoma (benign), and cyst. Previously, studies reported [46] measurement of oral tissue malignant using THz reflection imaging at frozen temperature and room temperature. The results demonstrated that the image contrast obtained at frozen temperature is better than the room temperature. The investigation of the tissue optical properties, say the absorption coefficient, the extinction coefficient, and the refractive index, is presented in this paper. Single cancer tissues were imaged using the reflex module's THz time-domain spectroscopy method. The tissue optical properties were compared to the histopathological findings. We hypothesize that there is a dominating component impacting the THz reflection signal other than water content to demonstrate the distinctions between normal and cancerous tissues. The obtained results show the effectiveness of using terahertz time-domain spectroscopy and imaging technologies to diagnose oral cancer and, hence, are clinically significant.

2. Methods and Materials

2.1. Samples. A single case of oral malignant, benign (ameloblastoma), and cyst specimens is collected from the pathologist between April 2019 and May 2020 who underwent an operation for oral melanoma. The institutional research board and the hospital ethical committee have approved our study protocol. The activities are carried out in compliance with the Helsinki Declaration's instructions. [47]. Further, the tissue is sliced into thin samples of $1.5\,\text{cm} \times 1.2\,\text{cm} \times 0.3\,\text{cm}$ in dimension and moved in for measuring using THz reflection spectroscopy.

2.2. Terahertz Pulsed Spectroscopy. Menlo Systems GmbH's Tera K15 THz-TDS equipment is utilized for the measurements. The arrangement is depicted schematically in Figure 1. A femtosecond laser generates 90 fs 1550 nm pulses at an 80 MHz rate, which excites the InGaAs semiconductor in the emitter photoconductive antenna (PCA), resulting in a picosecond pulse with a frequency range of

Table 1: Various noninvasive techniques for diagnosing oral tissues.

S.No	Techniques	Specimen	Sensitivity (%)	Advantages	Dis-advantages	Cost (INR)
1	Autofluorescence spectroscopy [13]	Oral tissue	91.1	It is a noninvasive technique and patient-friendly	Nonspecific	500–1000
2	Diffuse reflectance spectroscopy [14]	Oral tissue	94	Low cost, it gives quantitative results with good sensitivity & specificity	The result surrounds the overlapping of bands	500–2000
3	Elastic scattering spectroscopy biopsy [15]	Oral tissue	82	No secondary procedures	Time-consuming	
4	Histopathological examination [16]	Oral tissue	NA	The study of large portions of tissues minimal or risk	Chances of human error broader in scope Cell kinds are difficult to identify.	800–6400
5	Immunohistochemistry [17]	Oral tissue	NA	Used widely	Chances of human error	1500–3500
6	Incisional biopsy [18]	Oral tissue	NA	a little piece of tissue is used. Performed in suspected instances of cancer and precancer.	Increased risk of metastasis of malignant lesions.	1000–2000
7	Laser capture microdissection [19]	Oral tissue	NA	Cell separation is precise and fast	Expensive sample contamination. High level of expertise required	6000
8	Mass spectroscopy [20]	Oral tissue	NA	Molecular profiling of tissues	Expensive instrumentation	
9	Optical coherence tomography [21]	Oral mucosa	91	Noninvasive easy-to-use	Hyperkeratosis has a negative impact on image quality.	1000–2500
10	Raman spectroscopy [22]	Oral tissue	90	Minimal sample preparation nondestructive noninvasive	Bands overlap, making it difficult to distinguish specific components.	1500
11	Vital staining techniques [23]	Oral tissue	91	Noninvasive	A significant number of false positive instances are evaluated.	500

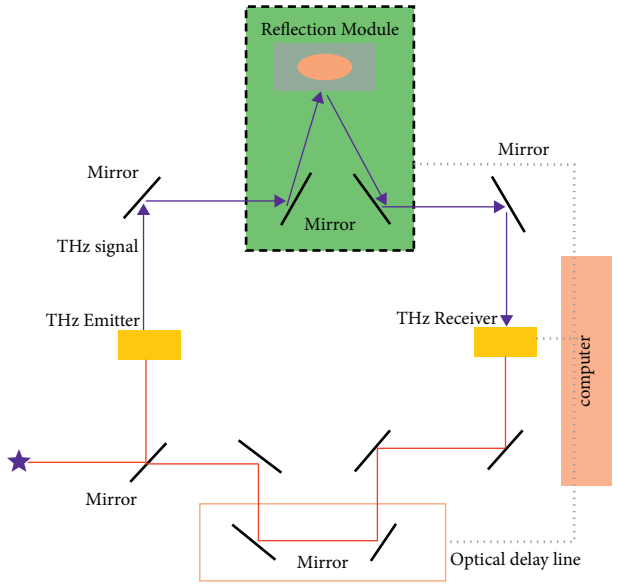

Figure 1: Typical experimental set-up of THz-TDS (reflection mode).

0.1 THz–2.5 THz. To concentrate the THz beam on the sample, two pairs of gold-coated off-axis parabolic reflectors were used.

Because of the nature of the THz signal (>10 W), a lock-in amplification (LIA) is used to separate it from the thermal history. Thermal background noise totally overshadows the

signals due to the THz-TDS method's coherent and gated detection. The delay line is controlled by a clock, which reads the lock-in amplification values at every single point and reports the terahertz pulsed waveforms. As predicted, the THz field's phase and amplitude data are received concurrently. The difference between the THz properties of the recorded samples defines the variance between the THz pulses generated, Eref, and THz-pulses transmitted [48].

2.3. Optical Parameter Extraction. As previously mentioned, the optical tissue characteristics of a specimen can be assessed by transmission or reflection. For media with a strong THz absorption coefficient, such as raw biological specimen, there is a tissue thickness limit for Terahertz-time domain spectroscopy in transmission geometry. Beyond the specified limit, reflection geometry can be used (Figure 1).

As shown in Figure 2(a), the terahertz signal is computed precisely as a function of time, and the frequency spectra of both the sample material signal and the reference signal (without sample) are produced using a numerical Fourier transformation. Further measurements on the obtained spectra offer information about the sample material under examination. As measurements are performed rather than intensity in the electric field, both amplitude and phase may be monitored at the same time. The absorption coefficient and the refractive index of tissues in the spectrum domain between 0.2 and 1.5 THz are depicted in Figures 2(a) and 2(b) of the spectral lines. Thus, the complex reflection coefficient is simply the Fresnel reflection coefficient [49].

$$\widetilde{R}_{\text{meas}} = \frac{\widetilde{S}_{R,\text{samp}}}{\widetilde{S}_{R,\text{ref}}} = R_{\text{meas}} e^{j\varnothing R} = \widetilde{R} = \frac{\widetilde{n}_R - 1}{\widetilde{n}_R + 1}. \tag{1}$$

Here, the reference signal $\widetilde{S}_{R,\text{the ref}}$ is obtained by using a metallic mirror instead of the sample, which is assumed to be a perfect reflector.

The value of the refractive index $\widetilde{n}_R = n_R - jk_R$ extracted from reflection measurement is directly calculated by inverting expression (1):

$$\begin{aligned} n_R &= \frac{1 - R_{\text{meas}}^2}{1 + R_{\text{meas}}^2 - 2R_{\text{meas}} \cos \varnothing_R}, \\ k_R &= -\frac{2R_{\text{meas}} \sin \varnothing_R}{1 + R_{\text{meas}}^2 - 2R_{\text{meas}} \cos \varnothing_R}. \end{aligned} \tag{2}$$

The primary disadvantage of reflection measurements is the inaccuracy introduced by even a slight misalignment of the reference mirror Δx concerning the sample position. This results in the following phase error:

$$\Delta_{\varnothing} = \frac{2\Delta x \omega}{c}. \tag{3}$$

And thus, errors on the extracted value of the refractive index

$$\begin{aligned} \frac{\Delta n_R}{n_R} &\approx k_R \Delta_{\varnothing} = \frac{2\omega K_R}{c} \Delta x = \alpha_R \Delta x, \\ \frac{\Delta k_R}{k_R} &\approx \text{abs}\left[\frac{\alpha_R}{2} - \frac{2\omega^2\left(n_R^2 - 1\right)}{c^2 \alpha_R}\right] \Delta x, \end{aligned} \tag{4}$$

where $\alpha_R = 2\omega K_R / c$ is the material's absorption coefficient. With regard to (4), the relative errors on the real and imaginary components of the complex refractive index change as the material becomes more absorbent. Indeed, the error introduced on n_R by the misalignment Δx grows larger as α_R rises, but the error made on k_R decreases until the absorption coefficient reaches $2\omega\sqrt{n_R^2 - 1/c}$.

As a result, for highly absorbing material, errors in the optical characteristics of the tested sample are relatively large and should be rectified numerically or experimentally [50]. Even though this methodology is imprecise, it enables the estimation of the refractive index of the absorbing material even in spectral bands with high absorption.

As shown in the following section, obtaining the frequency-dependent characteristics is slightly more difficult in reflection geometry than in transmission geometry. Similarly, all sample and the reference signals are captured during transmission. Further, the temporal shift is caused by the reference window content, an additional spatial shift occurs due to absorption, and the refraction data are stored within the measurement's phase detail, which is susceptible to devise artifacts. Additionally, there is another issue that arises due to the polarisation shift caused by reflection at a certain angle, which results in sample and the reference pulses being polarised differently. This is significant because the detector's sensitivity is polarization-dependent [51].

2.4. Limitation due to Formalin Fixing. Since the samples will be utilized in another study, formalin fixation must be conducted prior to THz measurements. This was not appropriate because, in addition to stiffening the samples, the fixation technique changes the terahertz characteristics of the tissues [52], which may induce tissue shrinkage. Our THz measurements would have a more difficult time identifying and comparing the reflections of distinct tissue layers as a result of the fixing technique. Given the positive results achieved using formalin-fixed samples despite these limitations, this investigation serves as a catalyst for further research employing fresh tissue samples.

3. Results and Discussion

3.1. Assessment of Tissue Optical Parameter and THz Spectroscopy Data. As seen in Figures 2(a)–2(e), it depicts the reflected THz pulses and their spectrum power levels in oral cancer tissue of various kinds, such as benign, malignant, and cyst.

Figure 2(a) explains the time domain waveform of oral malignant, benign, and cyst samples. In Figure 2(a), the graph **blue line** indicates the cyst sample. The cyst is the covering of the water lining. The **red line** indicates the

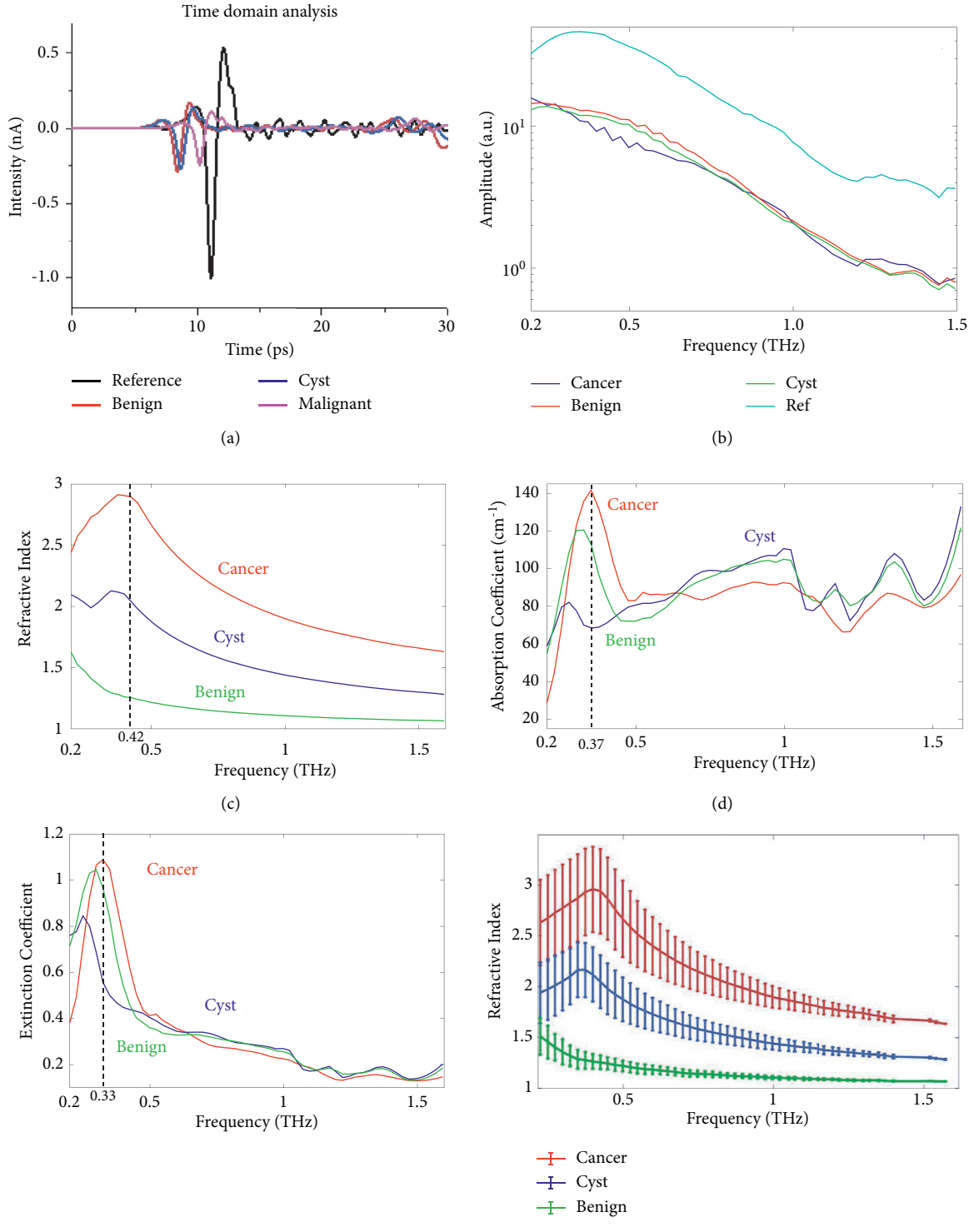

Figure 2: Continued.

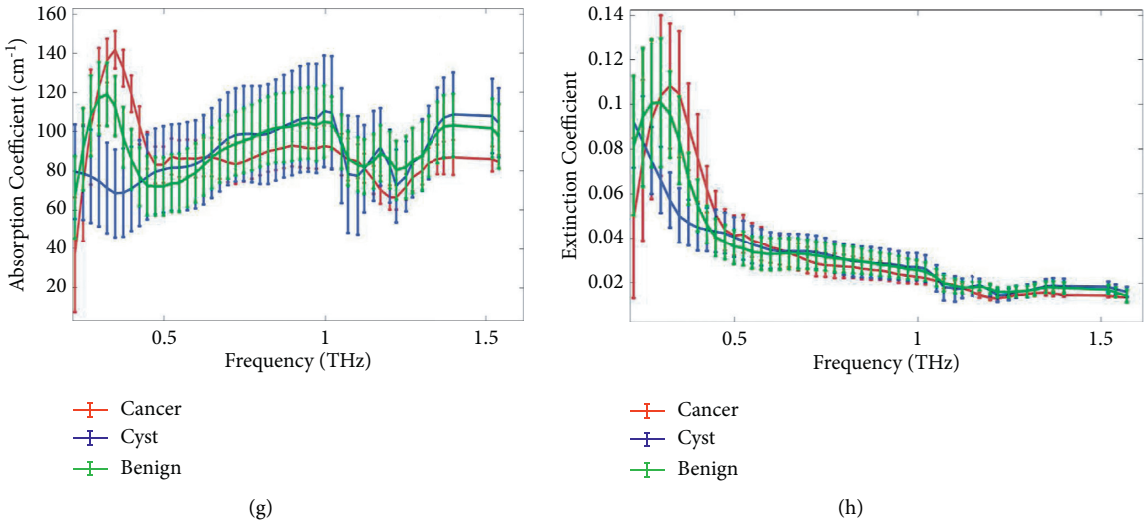

Figure 2: (a) The time-domain spectral line from the sample surface. (b) Frequency domain spectral lines passing through the sample surface. (c) Refractive index. (d) Absorption coefficient spectra. (e) Extinction coefficient spectra. (f) Mean refractive index of oral cancer, benign and cyst. (g) Mean absorption coefficient of oral cancer, benign and cyst. (h) Mean extinction coefficient of oral cancer, benign and cyst. The blue, red, and green lines indicate the oral squamous cell carcinoma, benign (ameloblastoma), and cyst, respectively.

benign sample, **the pink line** indicates the malignant sample, **and the black line** indicates the reference sample. The increase in the impulse function of oral malignant, benign, and cyst is subtle; the obvious difference is the peak altitude. The result emphasizes that there is a sufficient variation in tissue optic characteristics to be observed in geometry of reflection.

Figure 2(c) shows the difference in refractive index (n) of the oral cancer, benign, and cyst. The maximum spectra obtained from 0.2 to 0.3 THz are solely contributed not only by the water component, but also by the increased cell density.

Figures 2(d) and 2(e) present the calculated absorption coefficient (α) and the extinction coefficient of benign, malignant, and cyst samples. All absorption characteristics are followed by a distinct shift in the refractive index. Comparing the n and α spectra of benign, malignant, and cyst samples, the malignant sample shows higher absorption based on 10% of the water that is present in formalin-fixed samples. The presence of water with absorption is to be around 140 cm $^{-1}$ at 0.3 THz. It is likely understood that, along with water, the functional group like proteins or even the increased cell density plays a major role for the higher absorption spectra. The decrease in amplitude emphasizes the absorption of the sample from the beam's reflection via sample and their negligible losses.

Figures 2(f)–2(h) show the THz refractive index, absorption coefficient, and extinction coefficient of oral cancer, benign, and cyst samples. The error bars are overlapped, and the total error bar reflects a 95% confidence interval. Their THz absorption coefficient trend was most likely influenced by the liquid water in their tissues. In the frequency range of 0.2–0.5 THz, there is also a significant variance in tissue absorption coefficients, with the largest difference occurring for oral cancer at 140 cm^{-1} at 0.37 THz and 120 cm^{-1} for oral benign at 0.34 THz. The THz spectra of oral cancer, benign, and cyst are distinguishable in the frequency range of 0.2–0.5 THz.

Another factor that contributes to contrast in this study is tissue density, tumor microenvironment conditions (which are quite different from those of normal tissue, and undetermined cell division leading to increased cell density, as well as the presence of certain proteins). And this is linked to variations produced by cell modifications and aberrant protein density changes. The rise in vascularisation surrounding tumors, an increase in cell division and cell density, results in the release of growth factors.

The difference between the absorption coefficient and refractive index spectra of benign, cyst, and malignant samples is shown in greater detail in Figures 2(c) and 2(d). The disparity between two spectra is most significant at 0.42 THz. The increase in the variance at 0.42 THz is more likely to be caused by water interaction with a functional group such as proteins or increased cell/protein density alone [53].

3.2. Validation of Results. To perform this validation, formalin-fixed tissues were dehydrated by replacing the water with paraffin. Typically, tissues are preserved in 10% neutral formalin, and multiple ethanol solutions are used with increased concentration (say 70%, 80%, and 90%) to dehydrate the water from the sample. Following that, at a temperature of 60°C, the material was saturated with paraffin. Paraffin-embedded tissue bits were put out in specific moulds (regular plastic material with holes is utilized to better attach paraffin) and filled with molten paraffin at 60°C. The embedded paraffin at room temperature is then taken manually sectioned with a microtome to generate paraffin slices measuring 4-5 μm thick. Sections are then dewaxed. Finally,

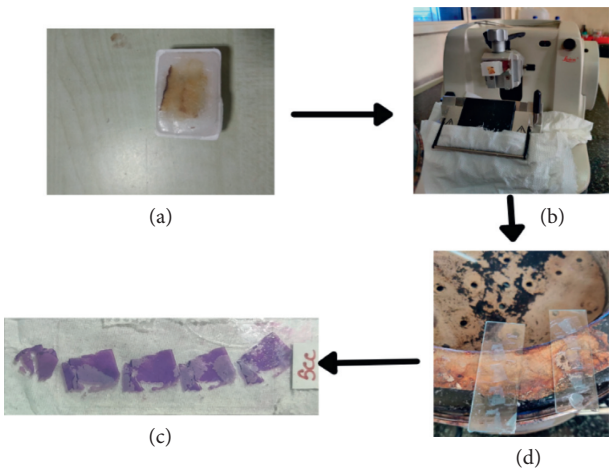

Figure 3: (a) Paraffin blocks with tissues. (b) Microtome. (c) Slide without stain. (d) Slide with H&E stain.

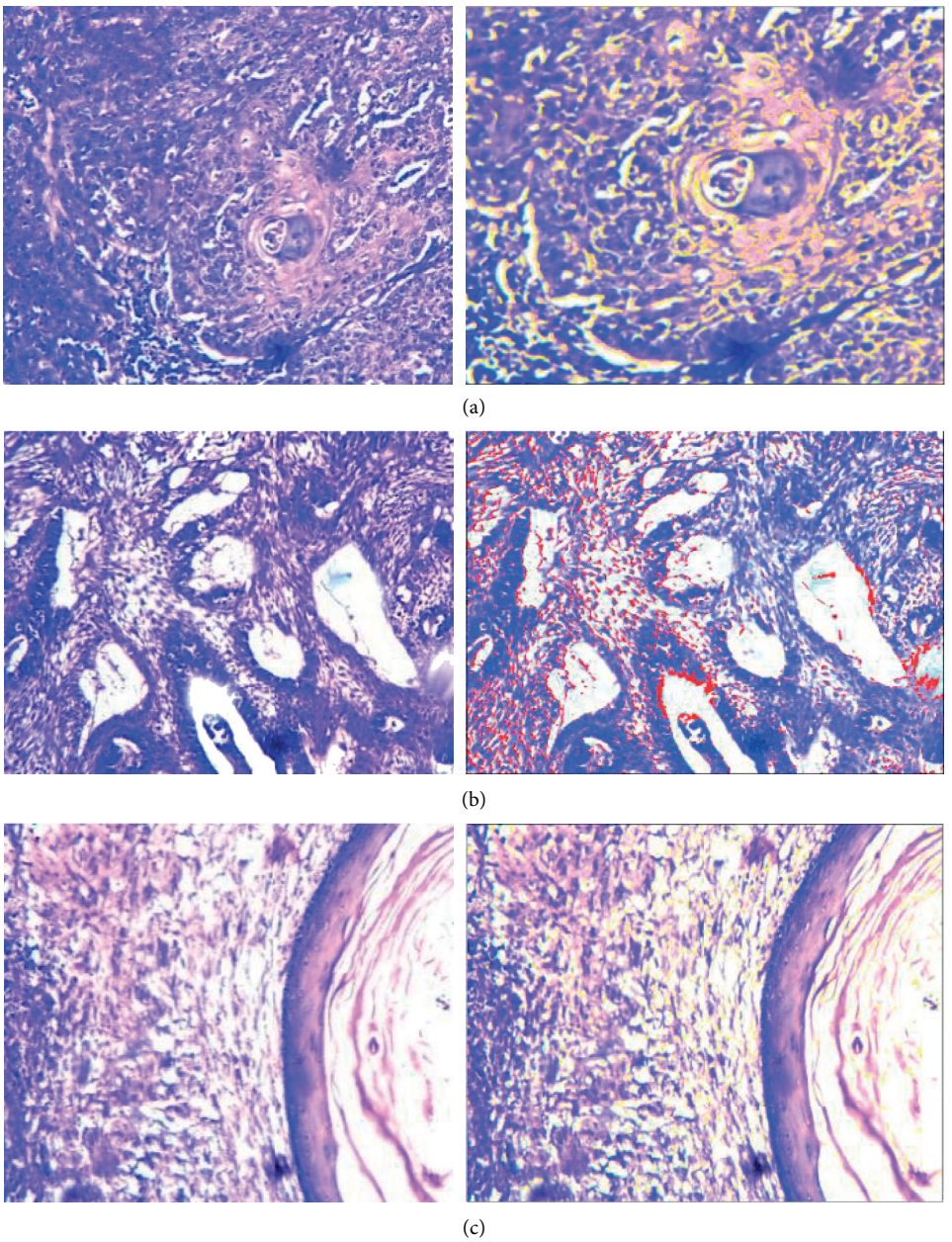

Figure 4: Cell nuclear recognition of H-E stained images. (a) Oral malignant. (b) Benign. (c) Cyst.

Table 2: Analysis report on H-E stained images.

Parameters	Malignant	Benign	Cyst
Cell nucleus	32.0078%	27.987%	17.11%
Cytoplasm	21.043%	48.013%	45.890%
Nonstained areas	46.9492%	24%	37%
Refractive Index (n)	2.8	2.1	1.6
Absorption coefficient (cm^{-1})	140	120	80

without immersing, thin sections were impregnated in glass slides, stained with haematoxylin and eosin (H & E), and evaluated under a light microscope as shown in Figure 3.

Haematoxylin is a standard stain dye used in this process; it gives the nuclei a bluish colour, while eosin (another stain dye used in histology) gives the cytoplasm and other tissue components a pinkish-orange stain [54]. To examine the differences between the benign, cyst, and cancerous tissues at the cellular level under the microscope, the cell density of cancer tissue is substantially high. At the same time, accelerated development of malignant/tumor cells set off considerable increases in tissue nuclei and often significantly more nucleoli in oral cancer cells [55, 56]. The result was tested using the image j software tool [57] by measuring the proportion of cell nucleus, cytoplasm per unit area of tissue. Nuclear recognition findings are seen in Figures 4(a)–4(c), and the proportions of each factor are calculated in Table 2. The findings indicate that the cancer tissue has almost double the number of nuclei than the healthier tissue, implying a significant rise in cell density. When the same cellular materials are used, a higher cell density often results in a higher refractive index and absorption coefficient.

Table 2 shows that as the internal cell density of malignant, benign, and cyst increases, the substantial increase in the refractive index and the absorption coefficient of malignant, benign, and cyst is observed. The internal density of the cell nucleus from cyst to malignant varies from 17% to 37%, whereas there occurs a higher reflected peak from cyst to malignant, i.e., 1.6 to 2.8, and absorption coefficient from cyst to malignant is $80\,cm^{-1}$ to $140\,cm^{-1}$.

However, to understand the detailed correlation between the cell density and the absorption coefficient, a large number of tissue samples for the clinical study are required. By overcoming the challenge in obtaining the multiple tissues, the future direction of this study can be formulated.

4. Conclusion

Terahertz spectroscopy can be utilized to distinguish oral malignant tumour from benign and cystic tissue since the estimated refractive indices and absorption coefficients were high in tumour tissues despite their comparatively low water content. This indicates that terahertz can help oral surgeons diagnose cancer tumor rapidly and correctly based on clinical distinctions observed in the lesions. THz can be utilized as an experimental generic technique for identifying oral cancer. Although this method will help new surgeons discover cancer lesions in formalin-fixed paraffin blocks, which is the gold standard for diagnosis, THz spectroscopy may be a helpful approach for noninvasive, effective intraoperative diagnosis of oral cancer, according to the current data.

Data Availability

The data are available upon request to the corresponding author.

Ethical Approval

The study was approved by institutional/regional/national ethics/committee/ethics board of SRMIST/1509/IEC/2018, and

Consent

Individual consent for this retrospective analysis was waived.

Conflicts of Interest

The authors declare that there are no conflicts of interest regarding the publication of this article.

References

[1] A. M. Manganaro, H. L. Hammond, M. J. Dalton, and T. P. Williams, "Oral melanoma," *Oral Surgery, Oral Medicine, Oral Pathology, Oral Radiology & Endodontics*, vol. 80, no. 6, pp. 670–676, 1995.

[2] M. J. Hicks and C. M. Flaitz, "Oral mucosal melanoma: epidemiology and pathobiology," *Oral Oncology*, vol. 36, no. 2, pp. 152–169, 2000.

[3] M. Mihajlovic, S. Vlajkovic, P. Jovanovic, and V. Stefanovic, "Primary mucosal melanomas: a comprehensive review," *International Journal of Clinical and Experimental Pathology*, vol. 5, pp. 739–753, 2012.

[4] Who.int.

[5] C. Laprise, H. P. Shahul, S. A. Madathil et al., "Periodontal diseases and risk of oral cancer in Southern India: results from the HeNCe life study," *International Journal of Cancer*, vol. 139, no. 7, pp. 1512–1519, 2016.

[6] A. C. Veluthattil, S. P. Sudha, S. Kandasamy, and S. V. Chakkalakkoombil, "Effect of hypofractionated, palliative radiotherapy on quality of life in late-stage oral cavity cancer: a prospective clinical trial," *Indian Journal of Palliative Care*, vol. 25, pp. 383–390, 2019.

[7] L. V. Galvão-Moreira and M. C. F. N. da Cruz, "Oral microbiome, periodontitis and risk of head and neck cancer," *Oral Oncology*, vol. 53, pp. 17–19, 2016.

[8] K. R. Atanasova and Ö. Yilmaz, "Looking in thePorphyromonas gingivaliscabinet of curiosities: the microbium, the host and cancer association," *Molecular Oral Microbiology*, vol. 29, no. 2, pp. 55–66, 2014.

[9] M. Fujita, H. Matsuzaki, Yanagi et al., "Diagnostic value of MRI for odontogenic tumours," *Dentomaxillofacial Radiology*, vol. 42, no. 5, Article ID 20120265, 2013.

[10] P. Palasz, L. Adamski, M. Gorska-Chrząstek, A. Starzynska, and M. Studniarek, "Contemporary diagnostic imaging of oral squamous cell carcinoma–a review of literature," *Polish Journal of Radiology*, vol. 82, pp. 193–202, 2017.

[11] H. M. Ayoub, T. L. Ayoub, G. B. Mccombs, and M. Bonnie, "The use of fluorescence technology versus visual and tactile

examination in the detection of oral lesions: a pilot study," *Journal of Dental Hygiene: JDH*, vol. 89, pp. 63–71, 2015.

[12] P. M. Lane, T. Gilhuly, P. Whitehead et al., "Simple device for the direct visualization of oral-cavity tissue fluorescence," *Journal of Biomedical Optics*, vol. 11, no. 2, p. 024006, 2006.

[13] D. C. G. De Veld, M. J. H. Witjes, H. J. C. M. Sterenborg, and J. L. N. Roodenburg, "The status of in vivo autofluorescence spectroscopy and imaging for oral oncology," *Oral Oncology*, vol. 41, no. 2, pp. 117–131, 2005.

[14] J. L. Jayanthi, G. U. Nisha, S. Manju et al., "Diffuse reflectance spectroscopy: diagnostic accuracy of a non-invasive screening technique for early detection of malignant changes in the oral cavity," *BMJ Open*, vol. 1, Article ID e000071, 2011.

[15] W. Jerjes, B. Swinson, K. S. Johnson, G. J. Thomas, and C. Hopper, "Assessment of bony resection margins in oral cancer using elastic scattering spectroscopy: a study on archival material," *Archives of Oral Biology*, vol. 50, no. 3, pp. 361–366, 2005.

[16] I. T. Dasc_alu, "Histopathological aspects in oral squamous cell carcinoma," *Open Access Journal of Dental Sciences*, vol. 3, 2018.

[17] G. Ulaganathan, Kt Mohamed Niazi, S. Srinivasan et al., "A clinicopathological study of various oral cancer diagnostic techniques," *Journal of Pharmacy & Bioallied Sciences*, vol. 9, pp. S4–S10, 2017.

[18] J. Kusukawa, Y. Suefuji, F. Ryu, R. Noguchi, O. Iwamoto, and T. Kameyama, "Dissemination of cancer cells into circulation occurs by incisional biopsy of oral squamous cell carcinoma," *Journal of Oral Pathology & Medicine*, vol. 29, no. 7, pp. 303–307, 2000.

[19] J. Muruganandhan, G. Sujatha, S. Patil, and A. T. Raj, "Laser capture microdissection in oral cancer," *The Journal of Contemporary Dental Practice*, vol. 19, pp. 475-476, 2018.

[20] R. Wang, Y. Yuan, Y. Zhou et al., "Screening diagnostic biomarkers of OSCC via an LCM-based proteomic approach," *Oncology Reports*, vol. 40, pp. 2088–2096, 2018.

[21] K. Bednarczyk, M. Gawin, M. Chekan et al., "Discrimination of normal oral mucosa from oral cancer by mass spectrometry imaging of proteins and lipids," *Journal of Molecular Histology*, vol. 50, no. 1, pp. 1–10, 2019.

[22] A. Malik, A. Sahu, S. P. Singh et al., "In vivo Raman spectroscopy-assisted early identification of potential second primary/recurrences in oral cancers: an exploratory study," *Head & Neck*, vol. 39, no. 11, pp. 2216–2223, 2017.

[23] H. Sreeshyla, U. Sudheendra, and R. Shashidara, "Vital tissue staining in the diagnosis of oral precancer and cancer: stains, technique, utility, and reliability," *Clinical Cancer Investigation Journal*, vol. 3, no. 2, p. 141, 2014.

[24] G. M. Png, J. W. Choi, B. W.-H. Ng, S. P. Mickan, D. Abbott, and X.-C. Zhang, "The impact of hydration changes in fresh bio-tissue on THz spectroscopic measurements," *Physics in Medicine and Biology*, vol. 53, no. 13, pp. 3501–3517, 2008.

[25] S. Huang, P. C. Ashworth, K. W. Kan et al., "Improved sample characterization in terahertz reflection imaging and spectroscopy," *Optics Express*, vol. 17, no. 5, pp. 3848–3854, 2009.

[26] S. Y. Huang, Y. X. J. Wang, D. K. W. Yeung, A. T. Ahuja, Y.-T. Zhang, and E. Pickwell-MacPherson, "Tissue characterization using terahertz pulsed imaging in reflection geometry," *Physics in Medicine and Biology*, vol. 54, no. 1, pp. 149–160, 2009.

[27] E. Pickwell and V. P. Wallace, "Biomedical applications of terahertz technology," *Journal of Physics D: Applied Physics*, vol. 39, no. 17, pp. R301–R310, 2006.

[28] D. H. Auston, "Picosecond optoelectronic switching and gating in silicon," *Applied Physics Letters*, vol. 26, no. 3, pp. 101–103, 1975.

[29] V. P. Wallace, D. A. Arnone, R. M. Woodward, and R. J. Pye, "Biomedical applications of terahertz pulse imaging," in *Proceedings of the Second Joint 24th Annual Conference and the Annual Fall Meeting of the Biomedical Engineering Society] [Engineering in Medicine and Biology*, pp. 2333-2334, Houston, TX, USA, October 2002.

[30] E. Pickwell, B. E. Cole, A. J. Fitzgerald, M. Pepper, and V. P. Wallace, "In vivostudy of human skin using pulsed terahertz radiation," *Physics in Medicine and Biology*, vol. 49, no. 9, pp. 1595–1607, 2004.

[31] R. M. Woodward, V. P. Wallace, D. D. Arnone, E. H. Linfield, and M. Pepper, "Terahertz pulsed imaging of skin cancer in the time and frequency domain," *Journal of Biological Physics*, vol. 29, no. 2/3, pp. 257–259, 2003.

[32] V. P. Wallace, A. J. Fitzgerald, E. Pickwell et al., "Terahertz pulsed spectroscopy of human basal cell carcinoma," *Applied Spectroscopy*, vol. 60, no. 10, pp. 1127–1133, 2006.

[33] P. C. Ashworth, E. Pickwell-MacPherson, E. Provenzano et al., "Terahertz pulsed spectroscopy of freshly excised human breast cancer," *Optics Express*, vol. 17, no. 15, pp. 12444–12454, 2009.

[34] A. J. Fitzgerald, V. P. Wallace, M. Jimenez-Linan et al., "Terahertz pulsed imaging of human breast tumors," *Radiology*, vol. 239, no. 2, pp. 533–540, 2006.

[35] G. Reese, C. Reid, R. Goldin et al., "Using terahertz pulsed imaging (TPI) to identify colonic pathology," in *Proceedings of the 2008 33rd International Conference on Infrared, Millimeter and Terahertz Waves*, Pasadena, CA, USA, September 2008.

[36] E. Pickwell, V. P. Wallace, B. E. Cole et al., "A comparison of terahertz pulsed imaging with transmission microradiography for depth measurement of enamel demineralisation in vitro," *Caries Research*, vol. 41, no. 1, pp. 49–55, 2007.

[37] E. Castro-Camus and M. B. Johnston, "Conformational changes of photoactive yellow protein monitored by terahertz spectroscopy," *Chemical Physics Letters*, vol. 455, no. 4-6, pp. 289–292, 2008.

[38] S. Ebbinghaus, S. J. Kim, M. Heyden et al., "An extended dynamical hydration shell around proteins," *Proceedings of the National Academy of Sciences*, vol. 104, no. 52, pp. 20749–20752, 2007.

[39] M. Walther, P. Plochocka, B. Fischer, H. Helm, and P. Uhd Jepsen, "Collective vibrational modes in biological molecules investigated by terahertz time-domain spectroscopy," *Biopolymers*, vol. 67, no. 4-5, pp. 310–313, 2002.

[40] G. J. Wilmink, B. L. Ibey, T. Tongue et al., "Development of a compact terahertz time-domain spectrometer for the measurement of the optical properties of biological tissues," *Journal of Biomedical Optics*, vol. 16, no. 4, Article ID 047006, 2011.

[41] I. Echchgadda, J. A. Grundt, M. Tarango et al., "Using a portable terahertz spectrometer to measure the optical properties ofin vivohuman skin," *Journal of Biomedical Optics*, vol. 18, no. 12, Article ID 120503, 2013.

[42] G. M. Png, R. Flook, B. W.-H. Ng, and D. Abbott, "Terahertz spectroscopy of snap-frozen human brain tissue: an initial study," *Electronics Letters*, vol. 45, no. 7, pp. 343-344, 2009.

[43] T. Bowman and M. El-Shenawee, "Terahertz spectroscopy for the characterization of excised human breast tissue," in *Proceedings of the 2014 IEEE MTT-S International Microwave Symposium (IMS2014)*, pp. 1–4, Tampa, FL, USA, June 2014.

[44] F. Wahaia, "Detection of colon cancer by terahertz techniques," *Journal of Molecular Structure*, vol. 1006, no. 1–3, pp. 77–82, 2011.

[45] D. Y.S. Chau, A. R Dennis, H. Lin, J. Axel Zeitler, and A. Tunnacliffe, "Determination of water content in dehydrated mammalian cells using terahertz pulsed imaging: a feasibility study," *Current Pharmaceutical Biotechnology*, vol. 17, no. 2, pp. 200–207, 2015.

[46] Y. C. Sim, K.-M. Ahn, J. Y. Park, C.-S. Park, and J.-H. Son, "Temperature-dependent terahertz imaging of excised oral malignant melanoma," *IEEE Journal of Biomedical and Health Informatics*, vol. 17, no. 4, pp. 779–784, 2013.

[47] M. Slaoui and L. Fiette, "Histopathology procedures: from tissue sampling to histopathological evaluation," *Methods in Molecular Biology*, vol. 691, pp. 69–82, 2011.

[48] O. Schubert, M. Hohenleutner, F. Langer et al., "Sub-cycle control of terahertz high-harmonic generation by dynamical Bloch oscillations," *Nature Photonics*, vol. 8, no. 2, pp. 119–123, 2014.

[49] M. Bernier, F. Garet, and J.-L. Coutaz, "Precise determination of the refractive index of samples showing low transmission bands by THz time-domain spectroscopy," *IEEE Transactions on Terahertz Science and Technology*, vol. 3, no. 3, pp. 295–301, 2013.

[50] E. M. Vartiainen, Y. Ino, R. Shimano, M. Kuwata-Gonokami, Y. P. Svirko, and K.-E. Peiponen, "Numerical phase correction method for terahertz time-domain reflection spectroscopy," *Journal of Applied Physics*, vol. 96, no. 8, pp. 4171–4175, 2004.

[51] F. Wahaia, I. Kašalynas, G. Valušis, C. D. C. Silva, and P. L. Granja, *Terahertz Spectroscopy for Gastrointestinal Cancer Diagnosis, Terahertz Spectroscopy-A Cutting Edge Technology Carvalho Silva and Pedro L. Granja (March 13th 2017)*, IntechOpen, London, UK, 2017.

[52] Y. Sun, B. M. Fischer, and E. Pickwell-MacPherson, "Effects of formalin fixing on the terahertz properties of biological tissues," *Journal of Biomedical Optics*, vol. 14, no. 6, Article ID 064017, 2009.

[53] C. Reid, A. P. Gibson, J. C. Hebden, and V. P. Wallace, "The use of tissue mimicking phantoms in analysingcontrast in THz pulsed imaging of biological tissue," in *Proceedings of the Conference Digest of the Joint 32nd International Conference on Infrared and Millimetre Waves, and 15th International Conference on Terahertz Electronics*, P. C. H. M. J. Griffin, T. J. Parker, and K. P. Wood, Eds., pp. 567-568, IEEE, Cardiff, UK, 2007.

[54] J. Black, *Microbiology: Principles and Exploration*, John Wiley & Sons, New York, NY, USA, 8th edition, 2012.

[55] S. Yamaguchi, Y. Fukushi, O. Kubota, T. Itsuji, T. Ouchi, and S. Yamamoto, "Origin and quantification of differences between normal and tumor tissues observed by terahertz spectroscopy," *Physics in Medicine and Biology*, vol. 61, no. 18, pp. 6808–6820, 2016.

[56] F. Wahaia, I. Kasalynas, D. Seliuta et al., "Study of gastric cancer samples using terahertz techniques," *Proceedings of SPIE*, vol. 9286, Article ID 92864H, 2014.

[57] C. A. Schneider, W. S. Rasband, and K. W. Eliceiri, "NIH Image to ImageJ: 25 years of image analysis," *Nature Methods*, vol. 9, no. 7, pp. 671–675, 2012.